

## Supplementary data

**Structural characterization and anti-osteoporosis activity of two polysaccharides from the rhizome of *Curculigo orchoides***

## Supplementary Tables

**Table S1**

The elution program of HPLC.

Time (min)	A%	B%	C%
0	0	17	83
24	0	17	83
25	0	19	81
30	0	18	82
31	5	14	81
32	5	14	81
33	0	18	82
34	5	14	81
36	0	18	82

A: ultrapure water

B: acetonitrile

C: 0.05 M phosphate buffer solution (pH 6.7)

**Table S2**

Static parameters of proximal tibia metaphysis.

<b>Group</b>	<b>Tb.Ar</b> <b>%</b>	<b>Tb.Th</b> <b>μm</b>	<b>Tb.N</b> <b>mm</b>	<b>Tb.Sp</b> <b>μm</b>
Sham	25.43±1.09	33775.52±1672.69	7.53±0.19	99042.21±2892.40
OVX	6.62±0.03##	33744.45±968.78	1.96±0.06##	475835.55±14803.72##
E2	16.71±0.13**	39008.64±1343.73**	4.29±0.17**	194433.24±7513.15**
CO50	16.94±0.65**	42674.52±483.83**	3.97±0.18**	209520.56±10915.22**

Values are expressed as mean ± SD. ##  $P < 0.01$  vs. Sham; \*\*  $P < 0.01$  vs. OVX.

**Table S3**

GC-MS analysis of COP50-1.

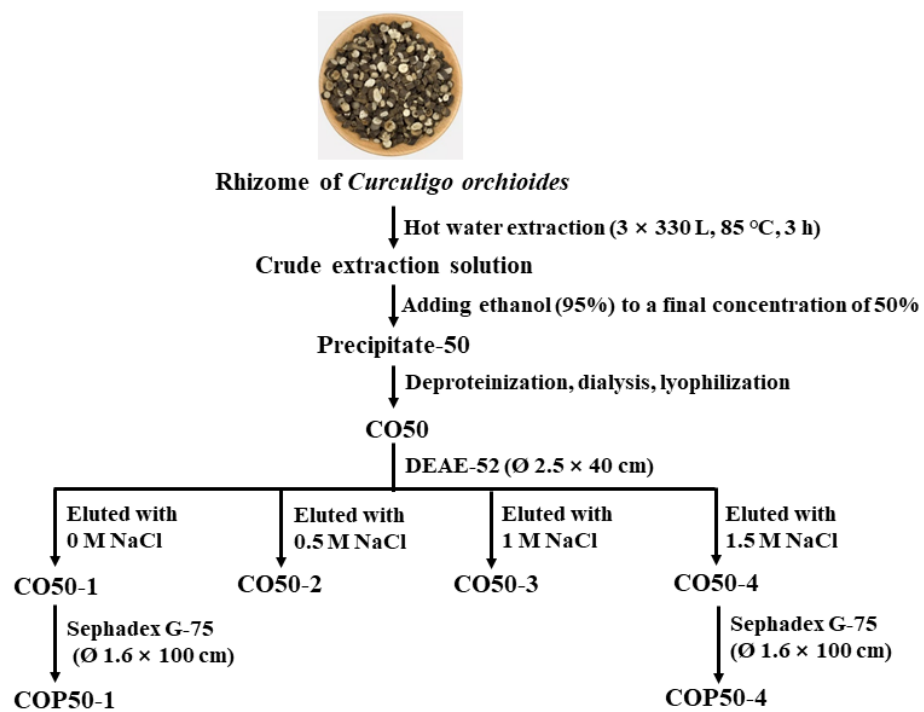
<b>t<sub>R</sub></b> <b>(min)</b>	<b>PMAA</b>	<b>Type of linkage</b>	<b>Relative Molar radio</b>	<b>Mass fragments (m/z)</b>
15.76	1,5-di- <i>O</i> -acetyl-2,3,4,6- tetra- <i>O</i> -methyl-D-glucitol	D-Glc <sub>p</sub> -(1→	4.5	43,59,71,87,101,117, 129,145,161,205
16.21	1,5-di- <i>O</i> -acetyl-2,3,4,6- tetra- <i>O</i> -methyl-D-galactitol	D-Gal <sub>p</sub> -(1→	2.2	43,59,71,87,101,117, 129,145,161,205
18.34	1,4,5-tri- <i>O</i> -acetyl-2,3,6-tri- <i>O</i> -methyl-D-glucitol	→4)-D-Glc <sub>p</sub> - (1→	6.1	43,57,71,87,99,117, 129,143,159,173,187, 203,233
19.24	1,3,4,5-tetra- <i>O</i> -acetyl-2,6- di- <i>O</i> -methyl-D-glucitol	→3,4)-D- Glc <sub>p</sub> -(1→	2.2	43,59,75,87,117,129, 143,161,185,203,233, 305
20.05	1,4,5,6-tetra- <i>O</i> -acetyl-2,3- di- <i>O</i> -methyl-D-glucitol	→4,6)-D- Glc <sub>p</sub> -(1→	2.1	43,57,75,85,101,117, 127,143,171,187,201, 231,261
20.18	1,4,5,6-tetra- <i>O</i> -acetyl-2,3- di- <i>O</i> -methyl-D-mannitol	→4,6)-D- Man <sub>p</sub> -(1→	1.0	43,57,75,85,101,117, 127,141,171,187,201, 231,261

**Table S4**

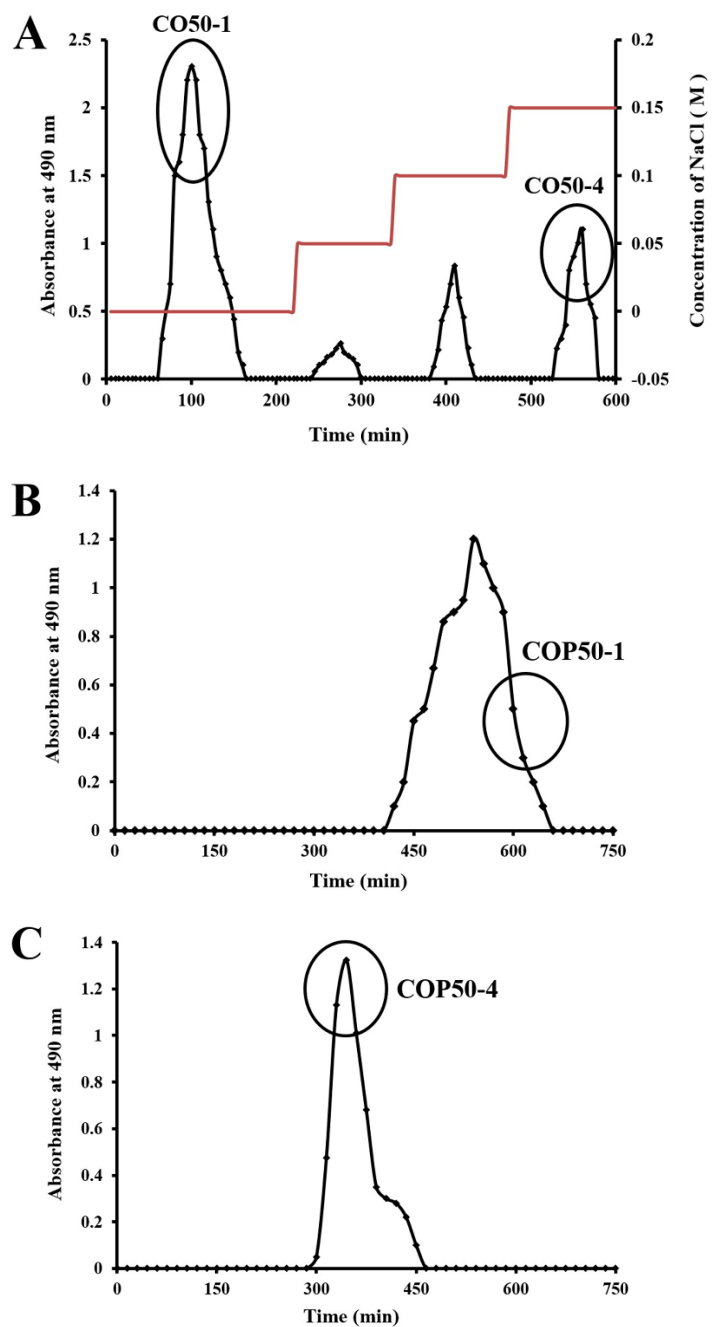
<sup>1</sup>H and <sup>13</sup>C NMR chemical shifts of COP50-1.

Glycosyl residue	H1	H2	H3	H4	H5	H6
	C1	C2	C3	C4	C5	C6
→4)- $\alpha$ -D-Glc $p$ -(1→	5.33	3.78	3.66	3.77	3.53	3.55/3.57
Residue A	99.5	72.8	75.1	76.9	73.7	60.7
$\alpha$ -D-Glc $p$ -(1→	5.32	3.76	3.69	3.55	3.57	3.52/3.53
Residue B	96.6	71.7	75.9	71.4	73.1	60.3
→3,4)- $\alpha$ -D-Glc $p$ -(1→	4.57	3.70	4.07	3.72	3.59	3.59/3.60
Residue D	95.7	72.9	78.8	76.1	73.0	62.5
→4,6)- $\alpha$ -D-Glc $p$ -(1→	4.90	3.77	3.65	3.71	3.61	3.76/3.78
Residue E	98.3	73.2	76.1	77.3	72.7	69.3
$\beta$ -D-Gal $p$ -(1→	4.56	3.88	3.56	3.71	3.67	3.34/3.36
Residue F	104.2	72.8	74.2	71.1	74.5	60.9
→4,6)- $\beta$ -D-Man $p$ -(1→	4.45	3.68	3.73	3.86	3.64	3.69/3.70
Residue G	102.6	72.9	73.4	76.0	74.5	69.4

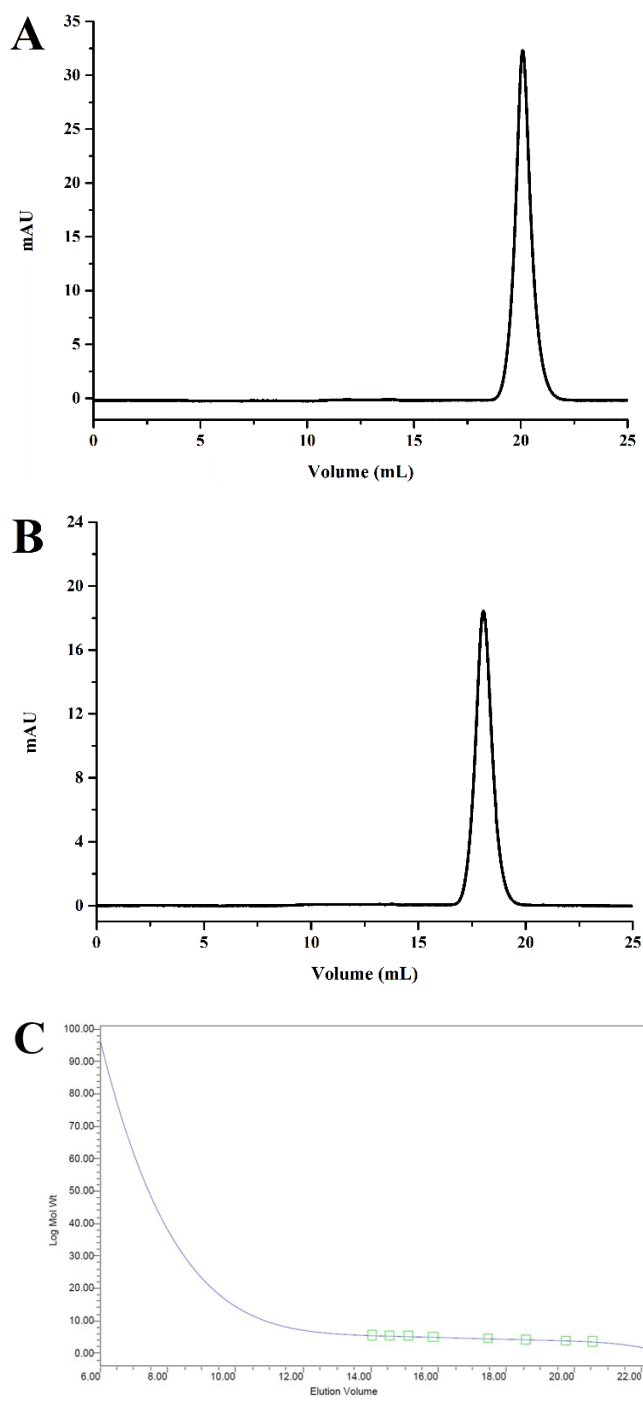
## Supplementary Figs



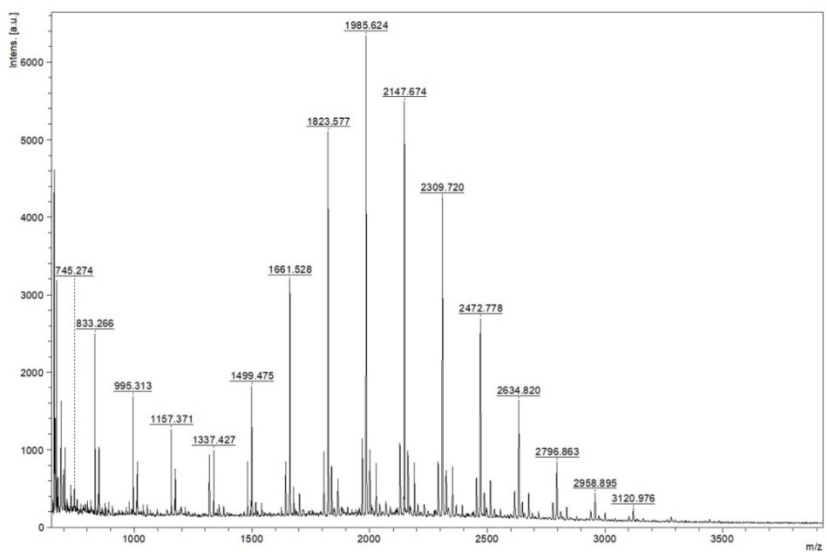
**Fig. S1** The flow diagram for the isolation and purification of polysaccharides from *Curculigo orchoides*.



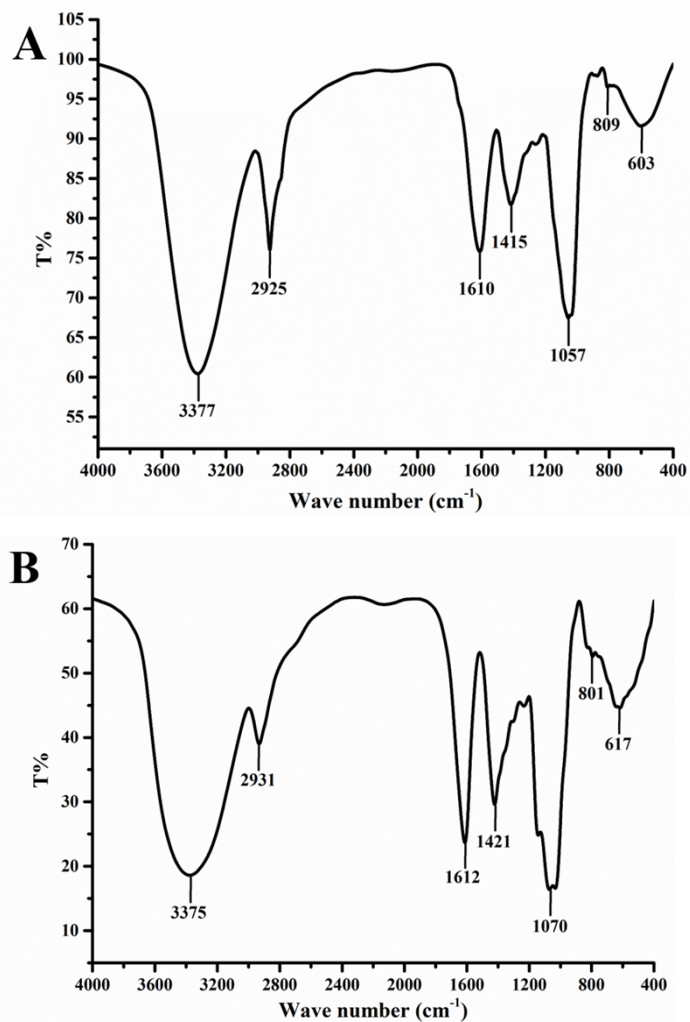
**Fig. S2** (A) Elution profile of CO50 on DEAE-cellulose 52 column. Elution profile of CO50-1(B) and CO50-4 (C) on Sephadex G-75 column.



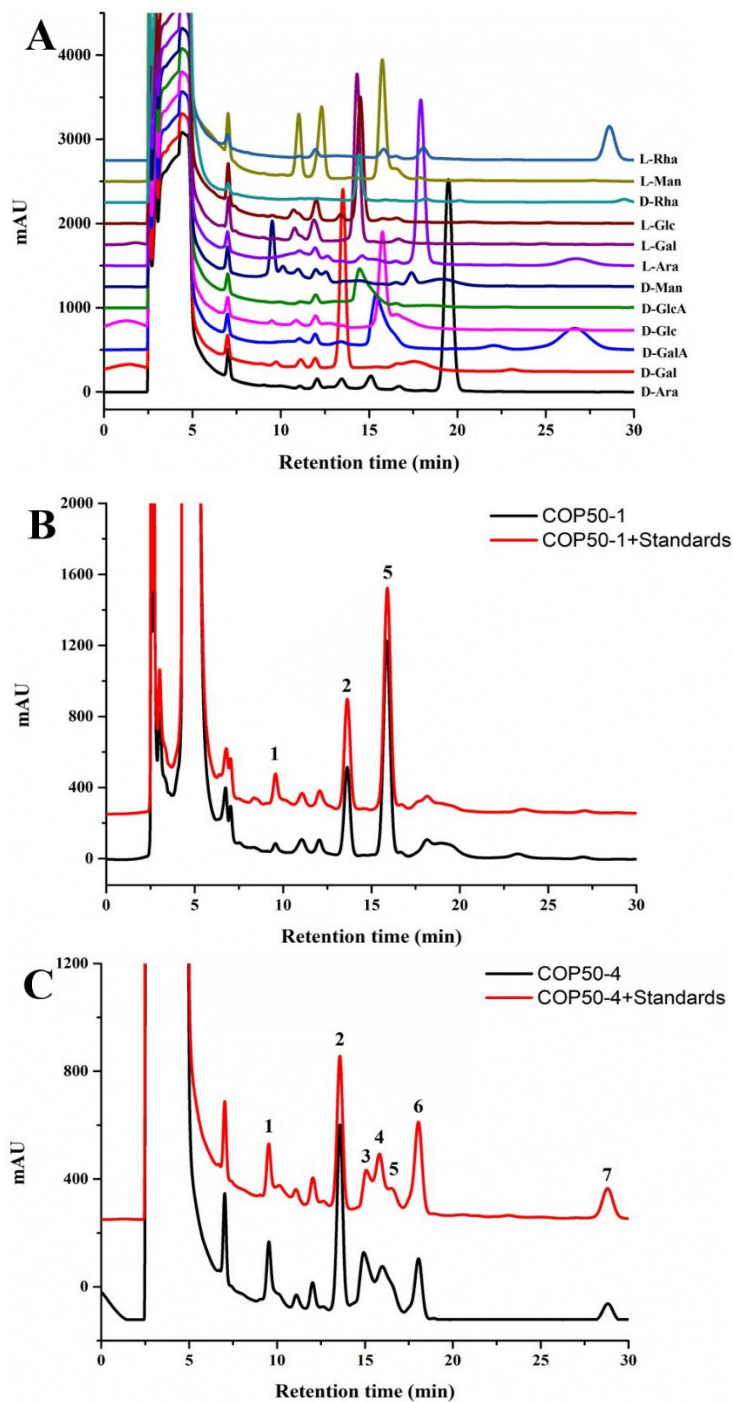
**Fig. S3** The HPGPC chromatogram of COP50-1 (A) and COP50-4 (B). (C) The calibration curve of HPGPC.



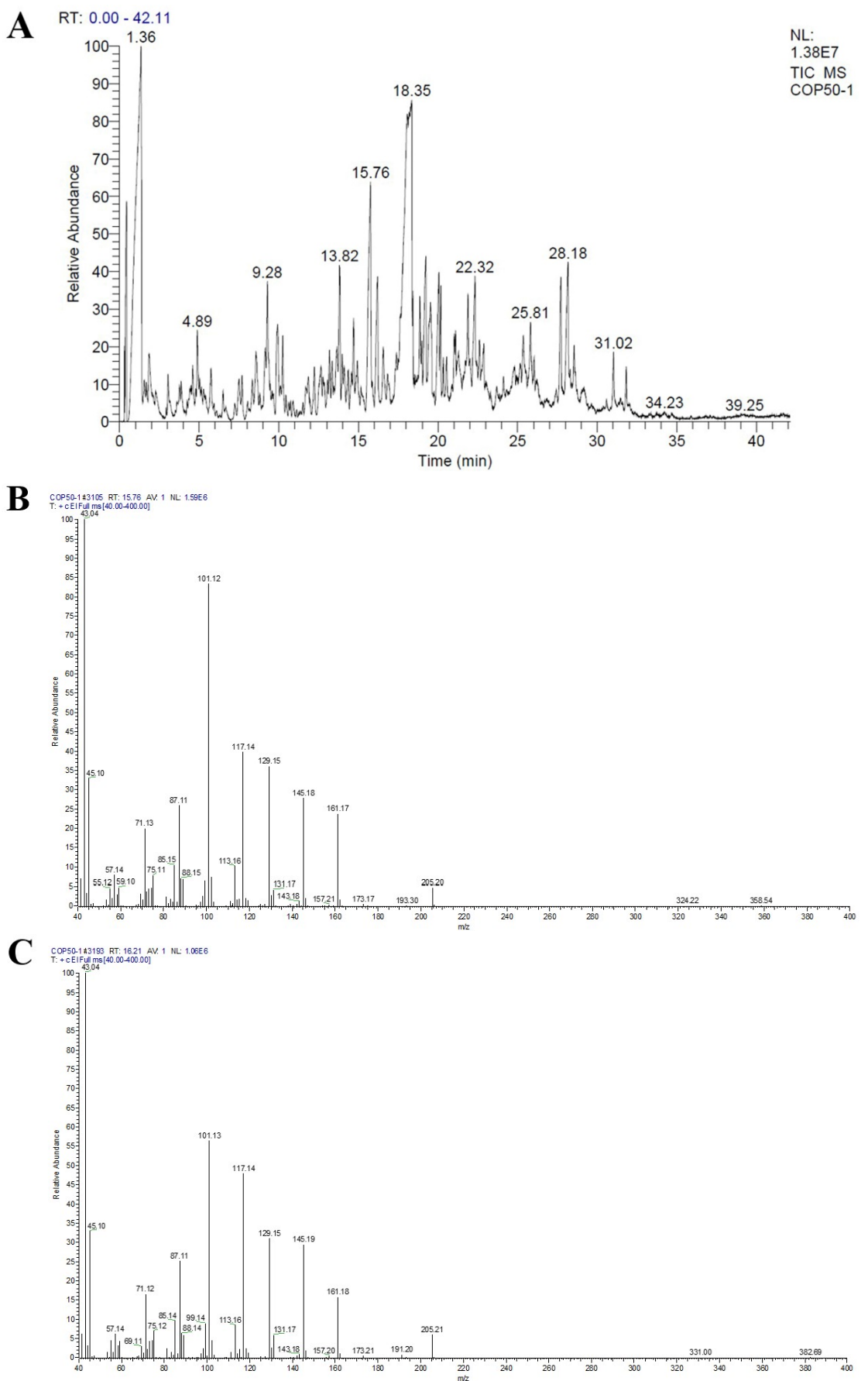
**Fig. S4** The MALDI-TOF-MS spectrum of COP50-1 in 500-4000 Da.

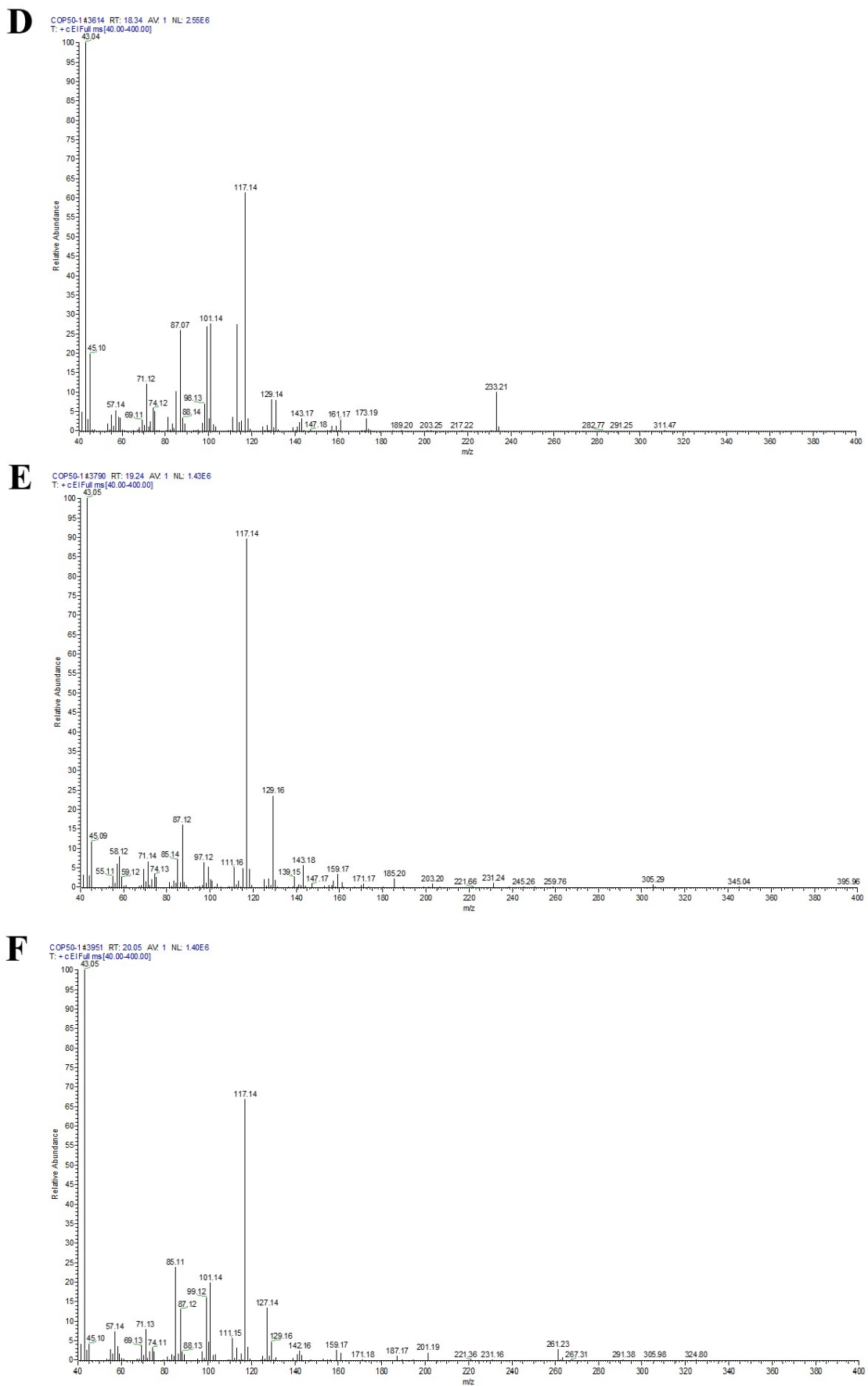


**Fig. S5** FT-IR spectra of COP50-1 (A) and COP50-4 (B).



**Fig. S6** HPLC chromatograms of (A) derivatives of standard monosaccharides, (B) COP50-1 derivatives and COP50-1 derivatives mixed with D-mannose, D-galactose, D-glucose and (C) COP50-4 derivatives and COP50-4 derivatives mixed with D-mannose, D-galactose, D-glucuronic acid, D-galactocuronic acid, D-glucose, L-arabinose, L-rhamnose.





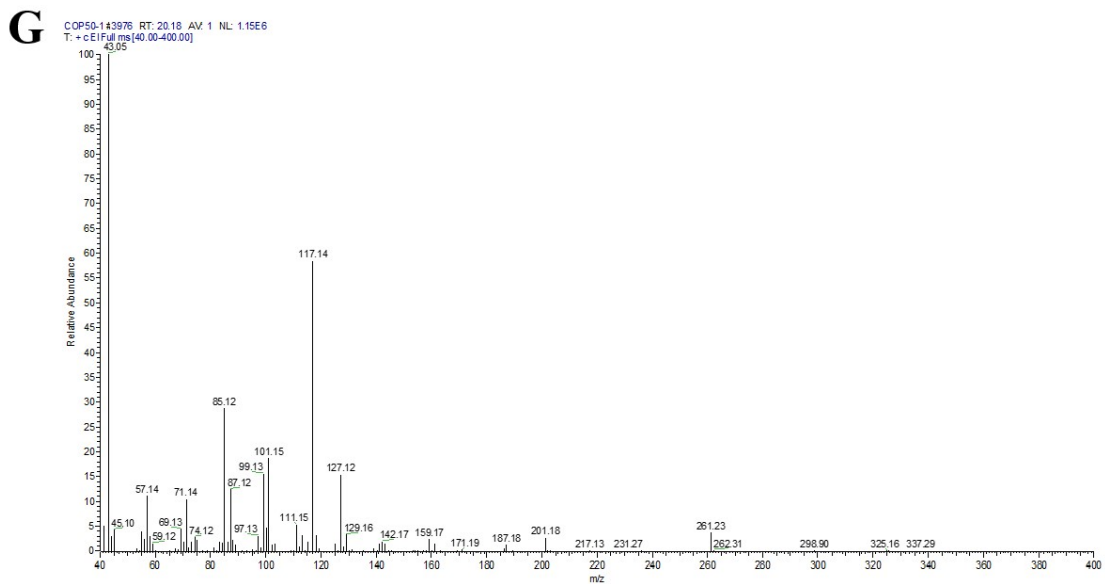


**Fig. S7 A:** The total ion chromatogram of COP50-1 derivates.

B: The mass spectrum of 1,5-di-*O*-acetyl-2,3,4,6-tetra-*O*-methyl-D-glucitol.

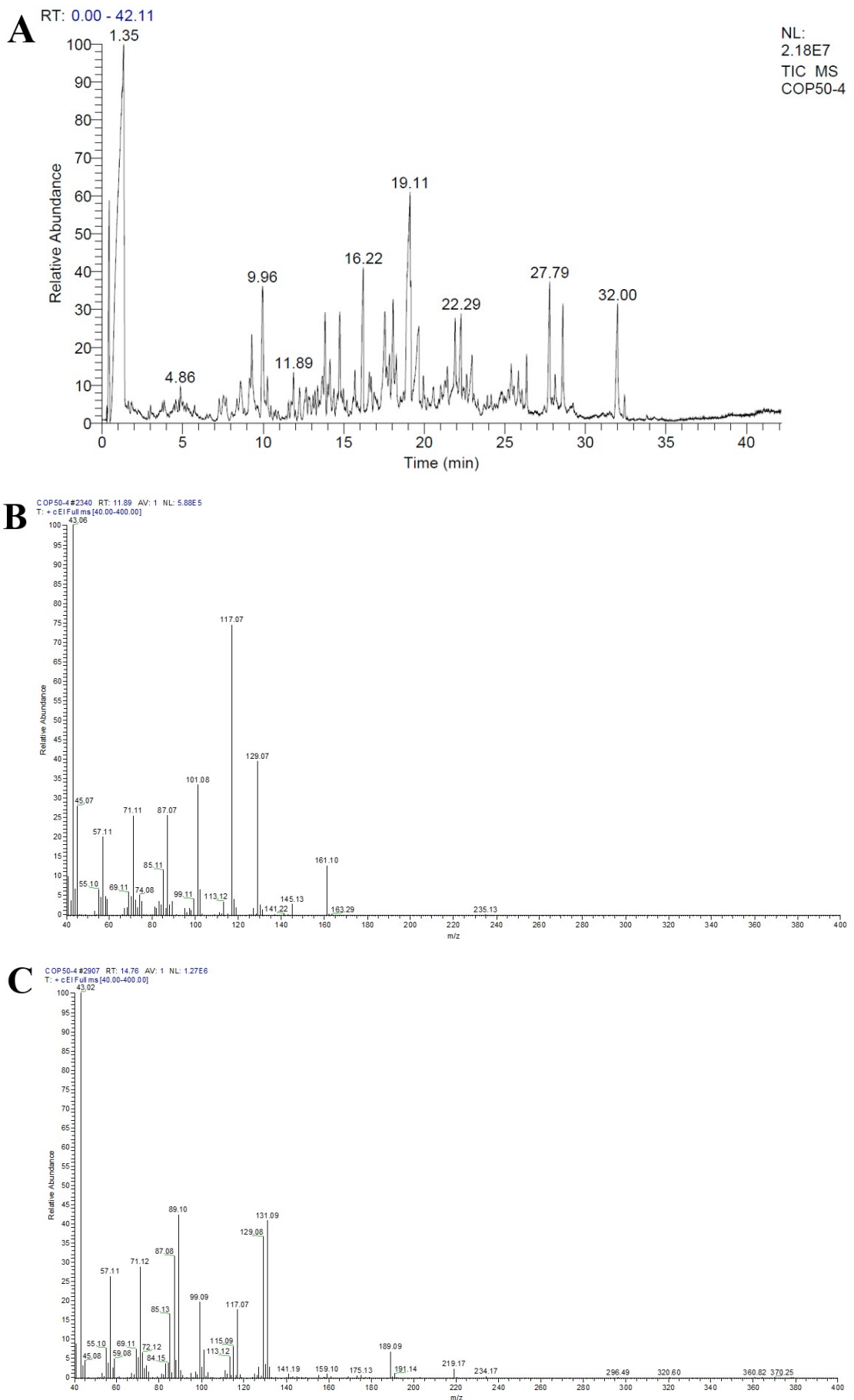
C: The mass spectrum of 1,5-di-*O*-acetyl-2,3,4,6-tetra-*O*-methyl-D-galactitol.

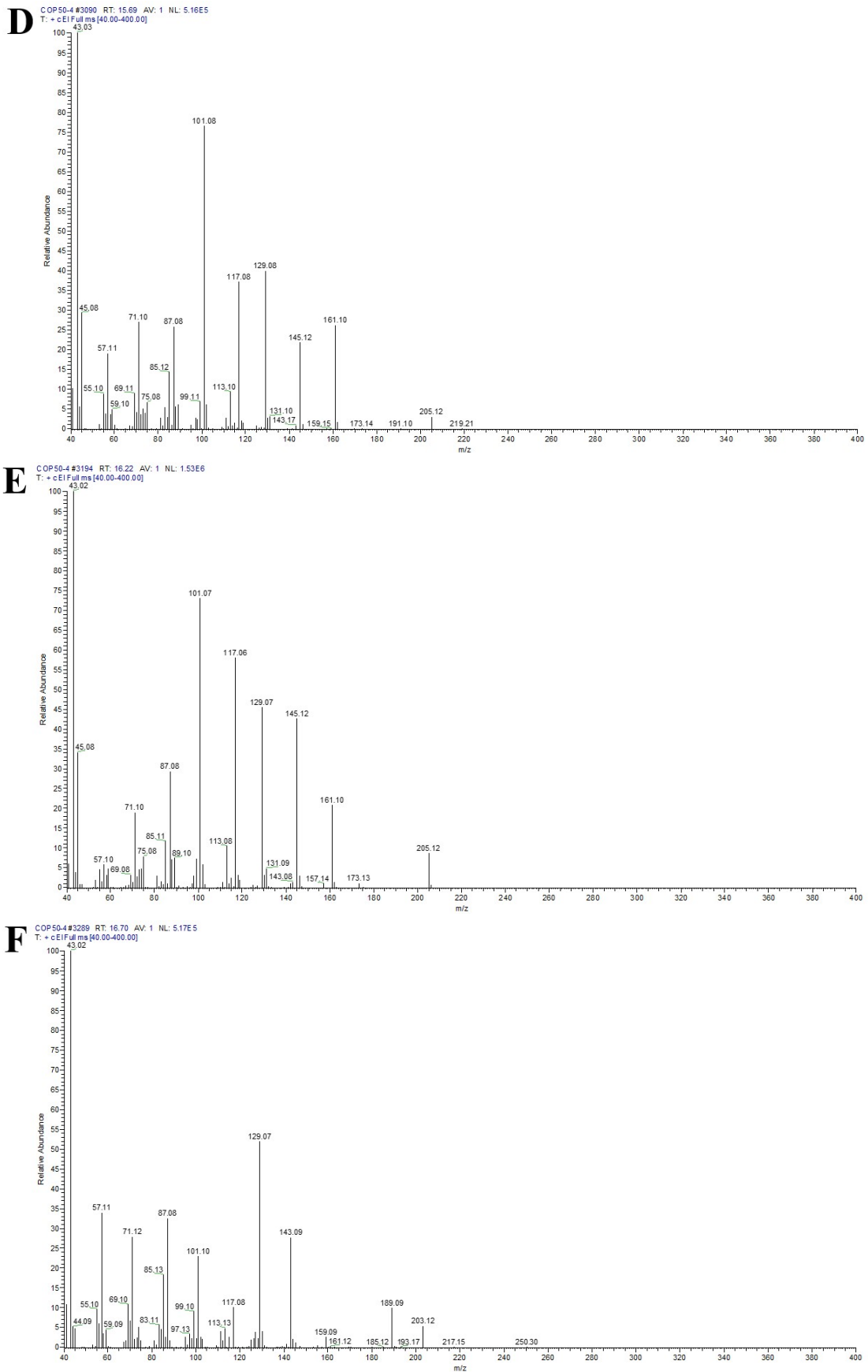
D: The mass spectrum of 1,4,5-tri-*O*-acetyl-2,3,6-tri-*O*-methyl-D-glucitol.

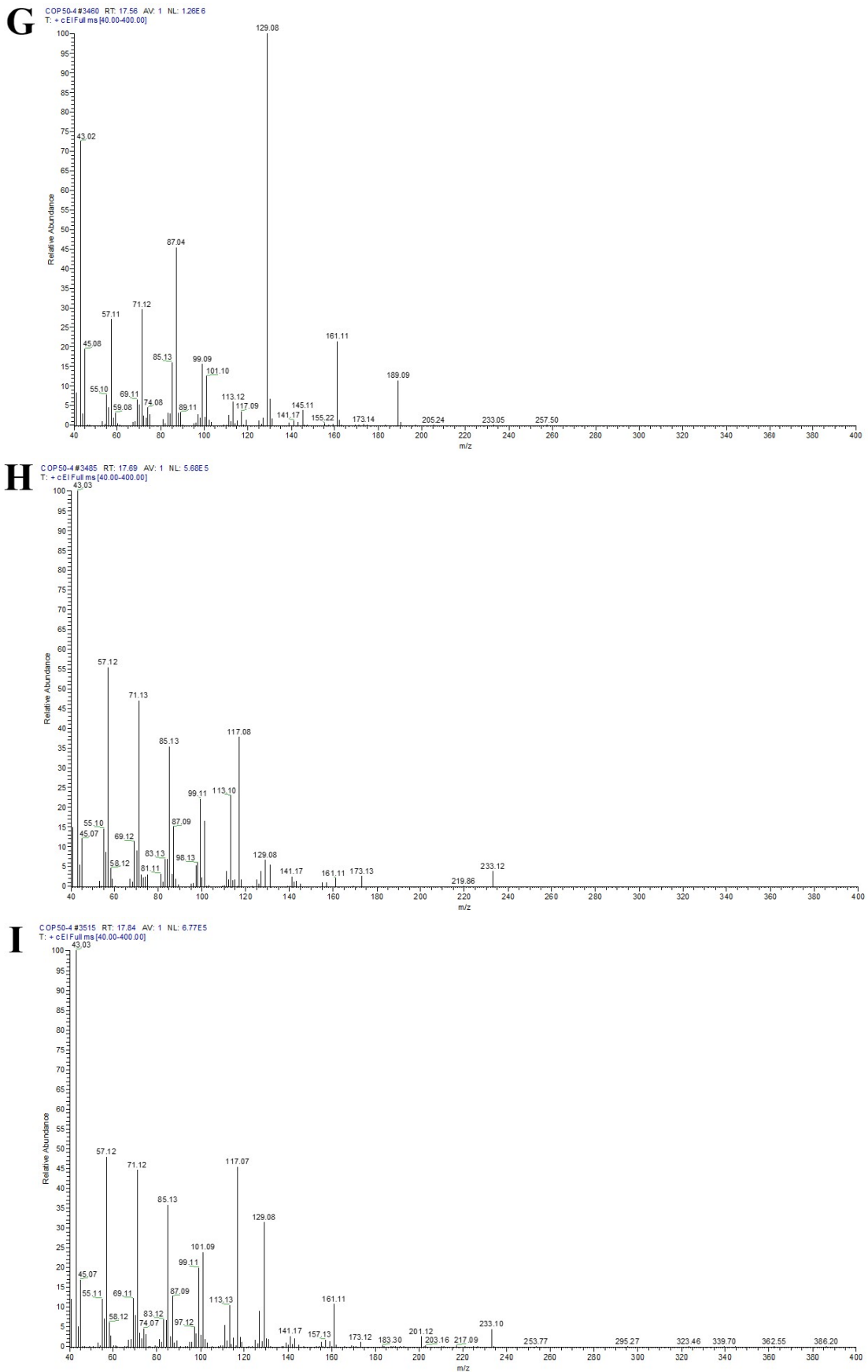
E: The mass spectrum of 1,3,4,5-tetra-*O*-acetyl-2,6-di-*O*-methyl-D-glucitol.

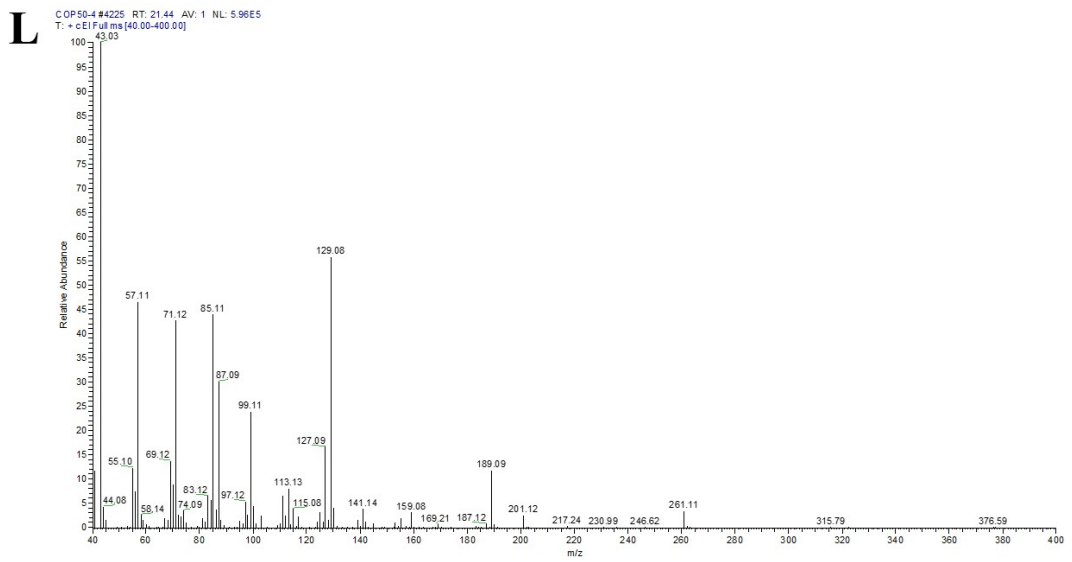
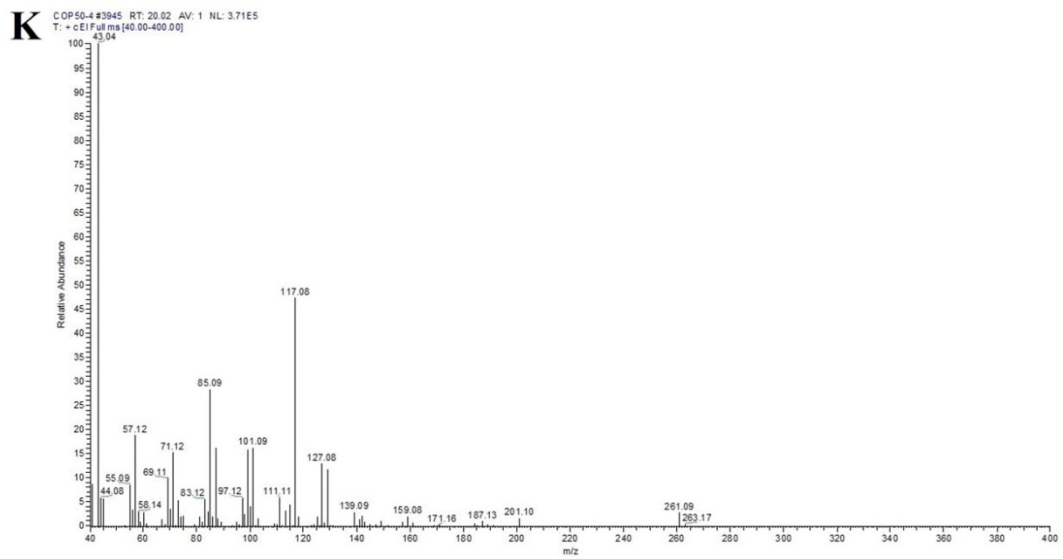
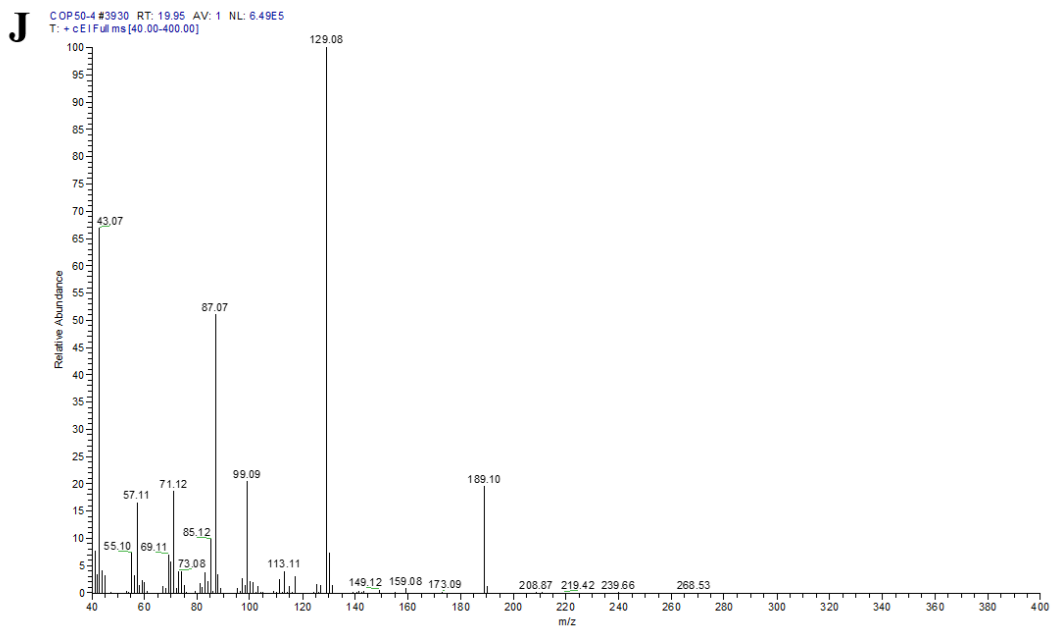
F: The mass spectrum of 1,4,5,6-tetra-*O*-acetyl-2,3-di-*O*-methyl-D-glucitol.

G: The mass spectrum of 1,4,5,6-tetra-*O*-acetyl-2,3-di-*O*-methyl-D-mannitol.









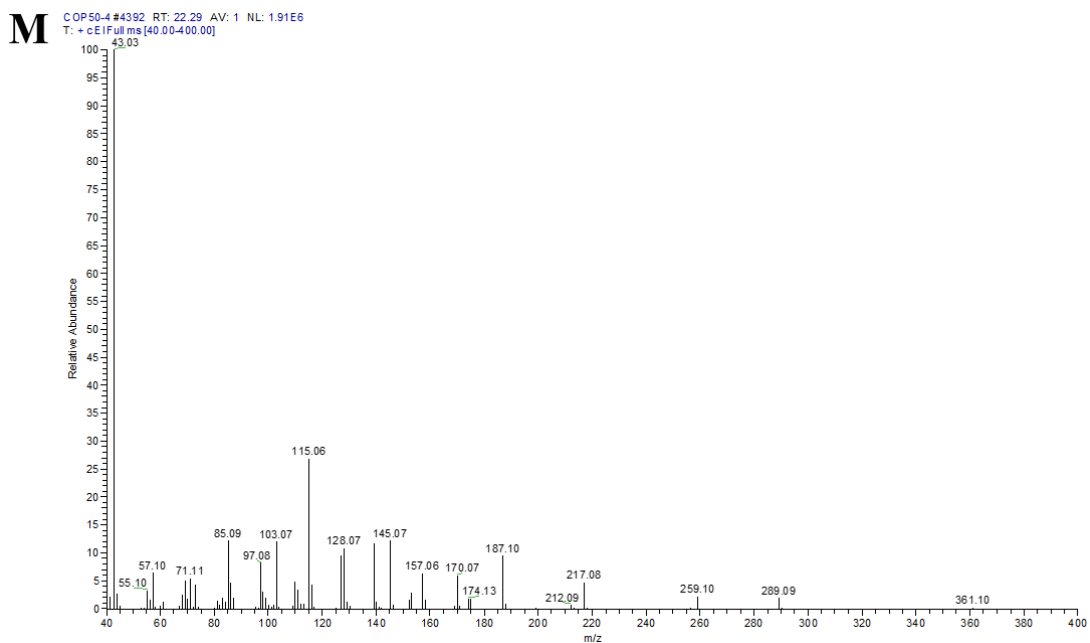


**Fig. S8 A:** The total ion chromatogram of COP50-4 derivates.

B: The mass spectrum of 1,4-di-*O*-acetyl-2,3,5-tri-*O*-methyl-L-arabinitol.

C: The mass spectrum of 1,2,5-tri-*O*-acetyl-6-deoxy-3,4-di-*O*-methyl-L-mannitol.

D: The mass spectrum of 1,5-di-*O*-acetyl-2,3,4,6-tetra-*O*-methyl-D-mannitol.

E: The mass spectrum of 1,5-di-*O*-acetyl-2,3,4,6-tetra-*O*-methyl-D-galactitol.

F: The mass spectrum of 1,2,4,5-tetra-*O*-acetyl-6-deoxy-3-*O*-methyl-L-mannitol.

G: The mass spectrum of 1,2,5-tri-*O*-acetyl-3,4,6-tri-*O*-methyl-D-mannitol.

H: The mass spectrum of 1,4,5-tri-*O*-acetyl-2,3,6-tri-*O*-methyl-D-glucitol.

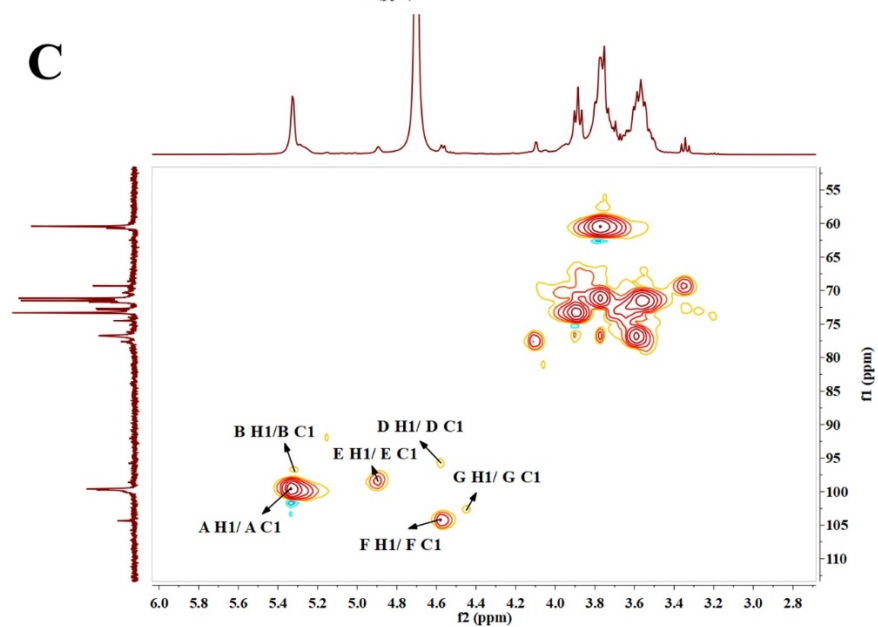
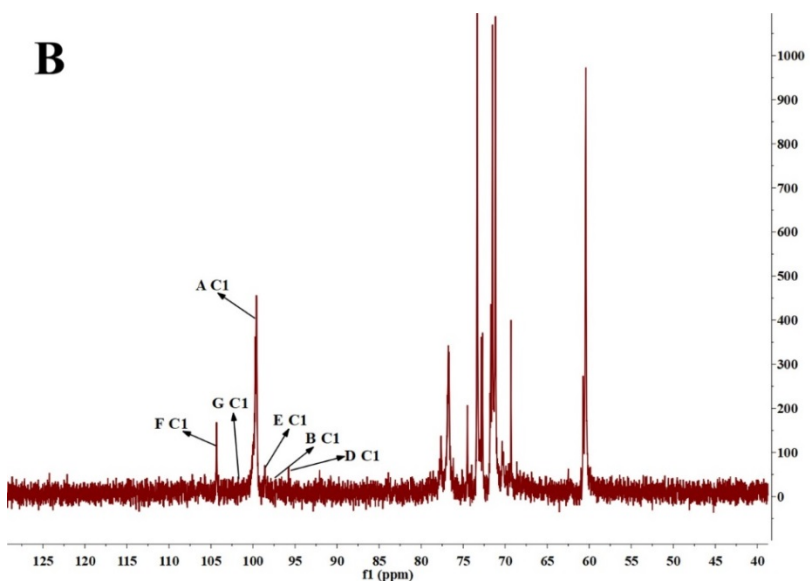
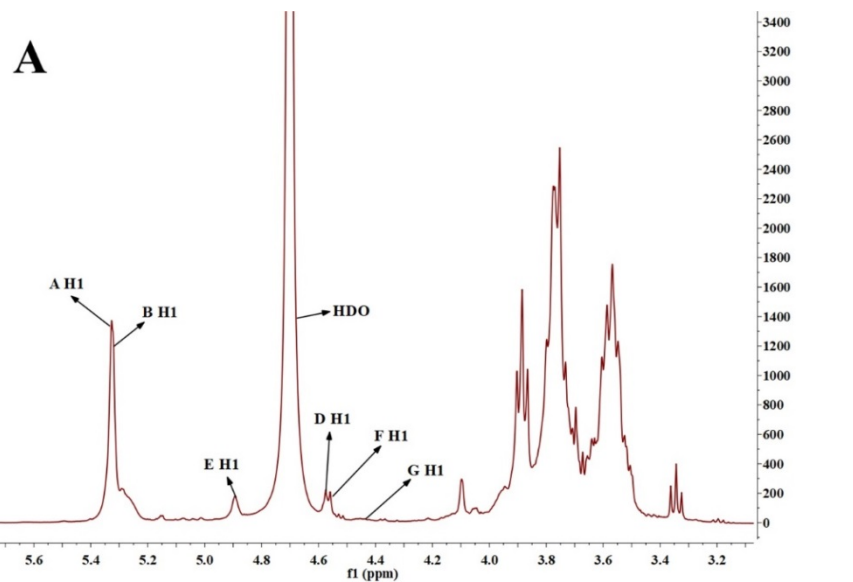
I: The mass spectrum of 1,3,5-tri-*O*-acetyl-2,4,6-tri-*O*-methyl-D-galactitol.

J: The mass spectrum of 1,2,4,5-tetra-*O*-acetyl-3-*O*-methyl-L-arabinitol.

K: The mass spectrum of 1,4,5,6-tetra-*O*-acetyl-2,3-di-*O*-methyl-D-galactitol.

L: The mass spectrum of 1,2,3,5,6-penta-*O*-acetyl-4-*O*-methyl-D-mannitol.

M: The mass spectrum of 1,2,3,4,5-penta-*O*-acetyl-L-arabinitol.



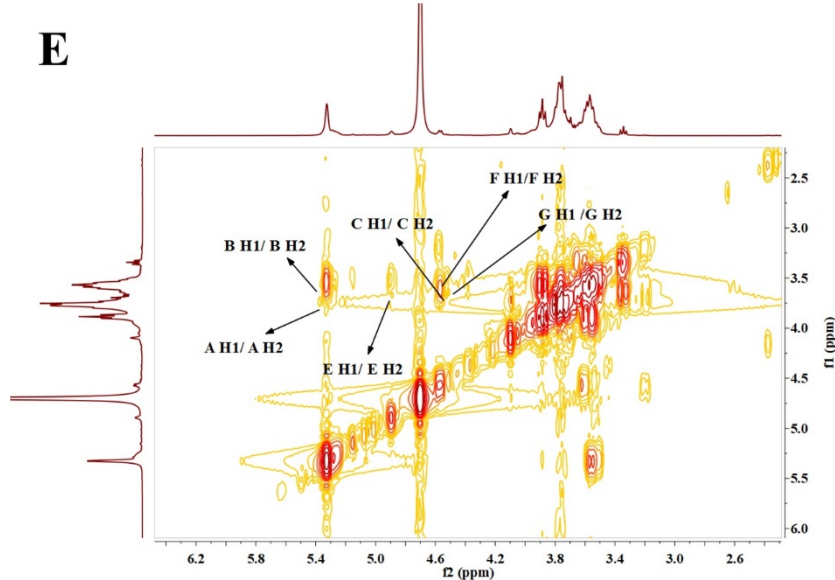
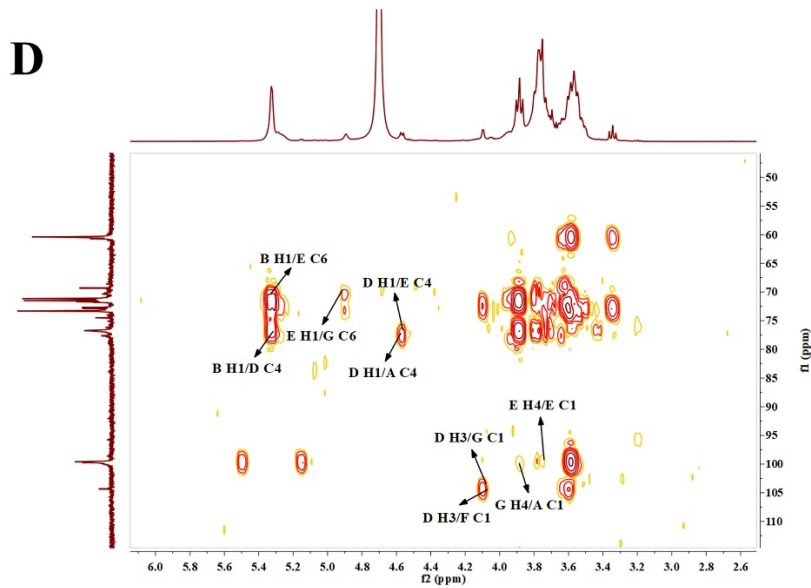


**Fig. S9** (A)  $^1\text{H}$ -NMR, (B)  $^{13}\text{C}$ -NMR, (C) HSQC, (D) HMBC, and (E)  $^1\text{H}$ - $^1\text{H}$  COSY spectra of COP50-1.

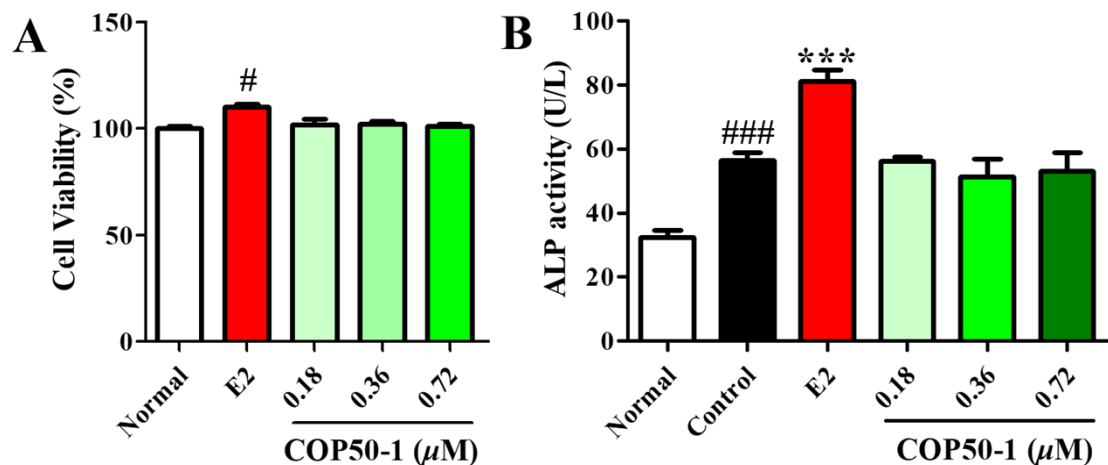


**Fig. S10** Effects of COP50-1 on the proliferation (A) and differentiation (B) of MC3T3-E1 cells. Values are mean  $\pm$  SEM.  $\#P < 0.05$ ,  $###P < 0.001$  vs. Normal.  $***P < 0.001$  vs. Control.